

Classical Print Reflection Models: A Radiometric Approach

Mathieu Hébert and Roger David Hersch[▲]

Ecole Polytechnique Fédérale de Lausanne (EPFL), Switzerland

The present contribution reviews the classical print prediction models of Williams and Clapper and of Clapper and Yule by pursuing a radiometric approach. The relationship between these models is established and the related respective contributions of Judd, Saunderson and Shore and Spoonhower are highlighted. Thanks to the radiometric approach, variants of the Williams and Clapper and Clapper and Yule models are derived in order to account for different measuring geometries (integrated sphere, $45^\circ/0^\circ$ geometry or other bistatic geometries) and for different reference white reflectors (coated paper, perfect white diffuser). The radiometric approach presented here gives a more profound understanding of these models and of the corresponding physical phenomena.

Journal of Imaging Science and Technology 48: 363–374 (2004)

Introduction

Color reproduction by printing images on paper results from the interaction of light with the printed paper. Light is partly reflected at the paper surface, partly absorbed by the inks, scattered within the paper bulk and partly internally reflected at the interface between the paper and the air. The study of the optical properties of the combination of paper, coating and inks is therefore crucial to ensure the quality of color reproduction. The aim of this article is to present and review the classical contributions in this field, by following a strict radiometric approach.

The first investigations about optical properties of prints dealt with photographic paper, where the paper is coated with gelatin. The gelatin coating is at the origin of the Fresnel internal reflection of light within the paper. In 1942, Judd published a table specifying the diffuse Fresnel reflectance at the gelatin-air interface, for several refractive indices of the coating material.¹ In 1952, Williams and Clapper proposed a model to predict the spectral reflectance of a Lambertian paper, coated with a uniform ink film, taking also into account internal reflections at the interface formed by the coating and the air.² It was developed for the classical $45^\circ/0^\circ$ measurement angles: the incident collimated beam illuminates the printed patch at an incidence angle of 45° , and the reflectance is measured according to the normal of the patch's surface, for a particular value of the refractive index of the gelatin. Recently, Shore and

Spoonhower³ have extended the Williams–Clapper model to any refractive index of the coating and for any angular measurement geometry including the integrating sphere geometry.

Most printed colors are produced by halftoning, where the ink is distributed on the paper as little ink dots according to given nominal coverage values. Simple models like the Murray–Davies model⁴ assume that between the dots the surface properties are those of the coated paper. In practice however, the light interacts both with printed and unprinted areas during its propagation within the paper. This phenomenon is called optical dot gain. In 1952, Clapper and Yule presented a model to predict the spectrum of a halftone print on paper, including the modeling of optical dot gain, taking into account multiple internal reflections and lateral scattering of light within the paper bulk.⁵ The Williams–Clapper² as well as the Clapper–Yule model⁵ are the starting points for a wide range of color prediction models.^{6,7}

In the present contribution, we study the interaction of light with a coated Lambertian substrate by relying on the laws of optics and by following the conventions of radiometry. We make the following assumptions:

- the substrate is a perfectly diffuse reflector,
- the refractive index of the substrate is the same as the refractive index of the coating, thereby avoiding any Fresnel reflection or refraction at the interface between the substrate (paper bulk) and the paper coating,
- the air-coating interface is a perfectly planar interface,
- the incident light is perfectly collimated and unpolarized.

Along this line of theoretical development we point out the respective contributions of Judd,¹ Williams and Clapper,² Saunderson,⁸ and Clapper and Yule,⁵ specifying and analyzing for each contribution its context and assumptions. Below, we introduce the basic notions of radiometry and optics such as radiant flux, radiance,

Original manuscript received November 1, 2003

▲ IS&T Member

mathieu.hebert@epfl.ch; Rd.hersch@epfl.ch

©2004, IS&T—The Society for Imaging Science and Technology

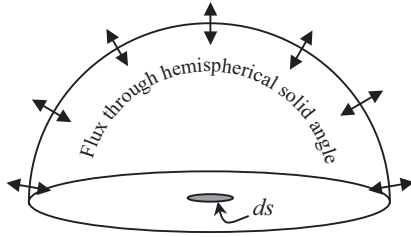


Figure 1. Irradiance is the flux relative to a surface element ds through the whole hemisphere.

irradiance, Lambertian reflector, Snell's laws, Fresnel formula and then derive the internal reflection of diffuse light on an interface¹ as well as its transmission through that interface. This allows us to derive the reflectance of a transparent solid layer located on top of a diffusely reflecting substrate. A straightforward extension yields the reflectance factor of a colored layer as derived by Williams and Clapper² and Shore and Spoonhower,³ both for freely selected illumination and viewing angles and for integrating sphere measuring geometries. Using the same radiometric approach, we derive the Clapper–Yule model⁵ and propose adaptations in order to account for the different measurement geometries and white references. We also highlight the simplifications underlying the Clapper–Yule model, in respect to the more rigorous Williams–Clapper model.

Elements of Radiometry

Modeling reflectances requires us to manipulate radiometric quantities and to take into account the geometry of the measurement device. We recall here definitions and properties⁹ necessary for the next sections. Note that each of the following quantities may be wavelength dependent.

Basic Definitions. We call *radiant flux* Φ the energy flowing through a surface per unit time.

The *irradiance* E (also called *brightness*) is the radiant flux per unit area that is incident on, passing through or emerging from a specified surface (Fig. 1). All directions in the hemispherical solid angle are to be included. For an element of radiant flux $d\Phi$ and a surface element of area ds ,

$$E^{(ds)} = d\Phi/ds. \quad (1)$$

A *solid angle* $d\omega$ formed by an area dA on a sphere of center S and radius x is said to be subtended by dA at point S and is defined as

$$d\omega = dA/x^2. \quad (2)$$

The infinitesimal surface dA is, according to geometric considerations (Fig. 2), $dA = x \sin\theta d\phi \cdot x d\theta$. Thus, the expression of the solid angle becomes

$$d\omega = \sin\theta d\theta d\phi. \quad (3)$$

The *radiant intensity* I is the radiant flux per unit solid angle that is incident on, passing through or emerging from a point in space and propagating in a specified direction. For an element of radiant flux $d\Phi$ through an element of solid angle $d\omega$

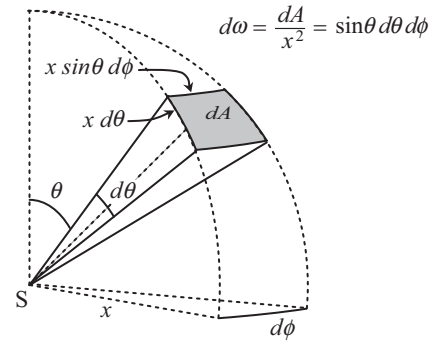


Figure 2. Solid angle $d\omega$ subtended by the projected area dA of the closed curve Γ at point S .

$$I^{(d\omega)} = d\Phi/d\omega. \quad (4)$$

The *radiance* L is the radiant flux per unit projected area and per solid angle that is incident on, passing through or emerging from a point in a specified surface (Fig. 3).

For an element of radiant flux $d^2\Phi$, relative to a surface element of area ds , contained within a solid angle $d\omega$ oriented according to direction (θ, ϕ) , the radiance $L^{(\theta, d\omega; ds)}$ is

$$L^{(\theta, d\omega; ds)} = \frac{d^2\Phi}{d\omega ds \cos\theta}. \quad (5)$$

By combining Eqs. (1) and (5), we obtain the relation between an *element of irradiance* $dE^{(ds)}$ and the radiance $L^{(\theta, d\omega; ds)}$, both relative to the same surface element ds and the same solid angle $d\omega$ around the same orientation (θ, ϕ) .

$$dE^{(ds)} = L^{(\theta, d\omega; ds)} \cos\theta d\omega \quad (6)$$

The relation between irradiance and radiance results from the integration of Eq. 6) over the hemisphere Ω

$$E^{(ds)} = \iint_{\Omega} L^{(\theta, d\omega; ds)} \cos\theta d\omega,$$

or, if we replace $d\omega$ by $\sin\theta d\theta d\phi$ (Eq. 3),

$$E^{(ds)} = \int_0^{2\pi} \int_0^{\pi/2} L^{(\theta, d\omega; ds)} \cos\theta \sin\theta d\theta d\phi. \quad (7)$$

Radiance Invariance. A light flux $d^2\Phi$ propagates between two elements of surface of respective area ds_1 and ds_2 and of respective normal N_1 and N_2 . Let us take a point P_1 on ds_1 and a point P_2 on ds_2 . The segment $[P_1P_2]$ of length x forms an angle θ_1 with respect to N_1 and an angle θ_2 with respect to N_2 . We call $d\omega_1$ the solid angle subtended by the projected area $ds_2 \cos\theta_2$ (area of the surface ds_2 projected onto the sphere of center P_1 and radius x) at point P_1 . Similarly, we call $d\omega_2$ the solid angle subtended by the projected area $ds_1 \cos\theta_1$ (area of the surface ds_1 projected onto the sphere of center P_2 and radius x) at point P_2 . According to this configuration (Fig. 4),

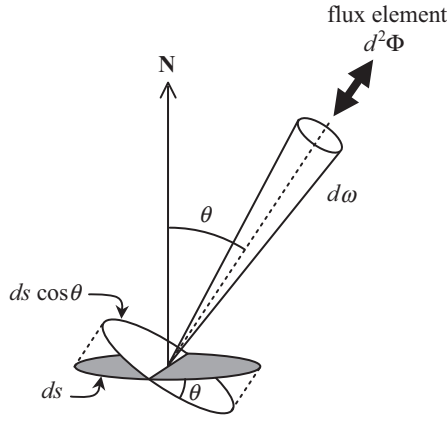


Figure 3. Radiance is the flux contained within an element of solid angle $d\omega$, oriented according to θ , and relative to the projected area $ds \cos \theta$ of the surface element ds .

$$d\omega_1 = \frac{ds_2 \cos \theta_2}{x^2} \text{ and } d\omega_2 = \frac{ds_1 \cos \theta_1}{x^2}. \quad (8)$$

We call L_1 the radiance defined at point P_1 by $d^2\Phi$, $d\omega_1$ and ds_1 (Eq. 5)

$$L_1^{(\theta_1, d\omega_1; ds_1)} = \frac{d^2\Phi}{d\omega_1 ds_1 \cos \theta_1}, \quad (9)$$

and we replace, according to Eq. (8), $d\omega_1$ and ds_1 by respectively $ds_2 \cos \theta_2 / x^2$ and $d\omega_2 x^2 / \cos \theta_1$. Therefore, Eq. (9) becomes

$$L_1^{(\theta_1, d\omega_1; ds_1)} = \frac{d^2\Phi}{d\omega_2 ds_2 \cos \theta_2} = L_2^{(\theta_2, d\omega_2; ds_2)}, \quad (10)$$

where L_2 is the radiance defined at point P_2 by $d^2\Phi$, $d\omega_2$ and ds_2 . The equality of L_1 and L_2 is known as the *radiance invariance property* [Ref. 9, p. 111], which is valid only if the light flux propagates without losses between ds_1 and ds_2 .

Reflectance. The reflective properties of the surface element, ds , can be characterized by the *reflectance* or the *reflectance factor* according to whether the radiometric quantities are normalized with a reference or not.

The *reflectance* ρ is the dimensionless ratio of the reflected flux $d\Phi_r$ to the incident flux $d\Phi_i$. If both fluxes are relative to the same element of surface ds , the reflectance is also the ratio of the reflected irradiance $E^{(ds)}$ to the incident irradiance $E_i^{(ds)}$

$$\rho = \frac{d\Phi_r}{d\Phi_i} = \frac{E^{(ds)} ds}{E_i^{(ds)} ds} = \frac{E^{(ds)}}{E_i^{(ds)}}. \quad (11)$$

The ratio $E^{(ds)}/E_i^{(ds)}$ defines a transmittance, τ , if $E^{(ds)}$ is the irradiance of the transmitted light.

The *reflectance factor* R is the ratio of the reflected flux $d\Phi$ to the flux $d\Phi_{ref}$ that would have been reflected by a perfectly diffuse surface under the same circum-

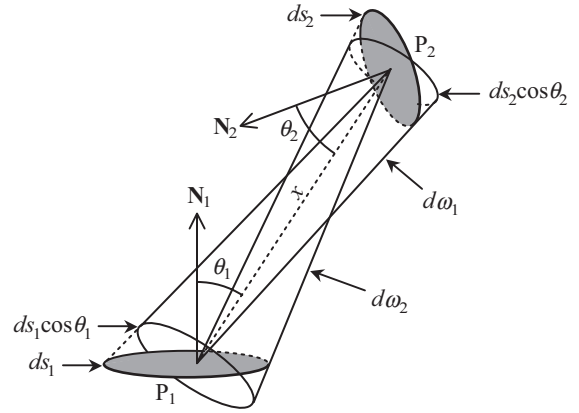


Figure 4. Light flux following a path between two elements of surface ds_1 and ds_2 .

stances (same illuminant of irradiance E_i , same surface element of area ds , same direction θ , same solid angle $d\omega_v$). According to that definition, R is also a ratio of irradiances, a ratio of radiances and a ratio of reflectances

$$R = \frac{d\Phi}{d\Phi_{ref}} = \frac{dE^{(ds)}}{dE_{ref}^{(ds)}} = \frac{L^{(\theta, d\omega_v; ds)}}{L_{ref}^{(\theta, d\omega_v; ds)}} = \frac{\rho}{\rho_{ref}}. \quad (12)$$

Note that if the reference reflectance is unity, the reflectance factor and the reflectance indicate the same dimensionless quantity. This may be the case when a photospectrometer is calibrated with a perfect diffuse white reflector. This may be one reason why the term “reflectance” is often used in the literature instead of the term “reflectance factor”.

Lambertian Emitters and Reflectors. The radiance $L^{(ds)}$ emitted by a perfectly diffuse emitter is independent of the direction of emission. Such emitters are called *Lambertian emitters* since the elements of radiance they reflect in each direction of the space verify Lambert’s cosine law (this property is a consequence of Eq. (6) with a constant radiance). According to Eq. (7), the irradiance emitted by a Lambertian emitter is

$$E^{(ds)} = L^{(ds)} \int_0^{2\pi} \int_0^{\pi/2} \cos \theta \sin \theta d\theta d\phi = \pi L \quad (13)$$

Similarly to Lambertian emitters, we define as *Lambertian reflectors* the perfect diffuse reflectors. They reflect a radiance $L^{(ds)}$ that is independent of the direction of observation, and an irradiance $\pi L^{(ds)}$. The reflectance of a Lambertian reflector is

$$\rho = \frac{\pi L^{(ds)}}{E_i^{(ds)}} \quad (14)$$

Measurement Geometry. According to the optical device used, the measuring device allows us to measure either a radiance or an irradiance.¹⁰ In this study, we consider two types of optical devices, in which the inci-

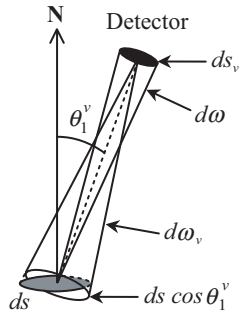


Figure 5. Radiance invariance between the detector and an element ds of the sample's surface.

dent light is a collimated beam. The first device is the integrating sphere, which receives light emerging from the print in every direction of the hemisphere, and therefore measures an irradiance. The second device is a detector of fixed area ds_v , receiving perpendicularly to its surface the light flux $d^2\Phi$ contained within a fixed solid angle $d\omega_v$. Such a detector measures the radiance L_v defined as (Eq. 5)

$$L_v = \frac{d^2\Phi}{d\omega_v ds_v}. \quad (15)$$

According to the radiance invariance property we can express the radiance captured by the detector equivalently in terms of radiance emerging from an element ds of the sample's surface

$$L_v = \frac{d^2\Phi}{d\omega ds \cos \theta_1^v}, \quad (16)$$

where ds is the element of the sample's surface that subtends the detector's radiance solid angle $d\omega_v$, $d\omega$ is the solid angle subtended by the detector's surface ds_v at a point of ds , and θ_1^v is the angle between the normal \mathbf{N} of ds and a segment linking one point of ds to one point of ds_v (Fig. 5).

In the following sections, the radiance captured by the detector will be defined by Eq. (16) rather than Eq. (15), i.e., we will consider the radiance emerging from the print through a surface element and a solid angle implicitly related to $d\omega_v$, ds_v and θ_1^v by the radiance invariance property.

The combination of an incident collimated beam (illumination or incidence angle θ_1^i) and a detector (viewing angle θ_1^v) is called θ_1^i / θ_1^v *measurement geometry*. Classical devices are based on the $45^\circ/0^\circ$ geometry: a collimated light beam illuminates a small area ds of the surface, with an angle of 45° in respect to the normal \mathbf{N} of the surface (Fig. 6). The detector receives the light emerging from the sample along \mathbf{N} .

Optics of a Planar Interface Between Two Transparent Media

In this section, we consider a planar interface, of normal vector \mathbf{N} , made of two transparent, i.e., non absorbing, media of respective refractive indices n_1 and n_2 . The subscript 1 is relative to air, and the subscript 2 is

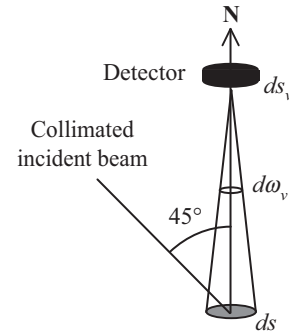


Figure 6. Configuration of a measuring device for a $45^\circ/0^\circ$ measurement geometry.

relative to the coating. The superscripts i and v denote incident and viewing angles.

Snell's Laws and Fresnel Formulae. A ray of light falling onto the interface with an incidence angle θ_1 is partially reflected by and partially transmitted through the interface (Fig. 7). Snell's first law insures that the incident, the reflected and the refracted rays belong to a same plane containing the surface normal vector \mathbf{N} . According to Snell's second law, the reflected ray propagates into the specular direction, so that the reflected ray and the incident ray make the same angle θ_1 with the normal \mathbf{N} . The transmitted ray is refracted and propagates in the medium 2 with an angle θ_2 with respect to $-\mathbf{N}$, related to θ_1 by Snell's third law¹¹

$$\sin \theta_2 = \left(\frac{n_1}{n_2} \right) \sin \theta_1. \quad (17)$$

The ratio of reflected to incident fluxes, called *Fresnel reflection factor*, is determined by Fresnel's formulae¹¹ as a function of the angles θ_1 and θ_2 , where θ_2 is derived from Eq. (17) for a given relative refractive index n_1/n_2 . The reflection factor is also defined as the ratio of the reflected to incident intensities. Both this definitions are equivalent since the incidence and reflection solid angles are equal. For non-polarized light,

$$r_{n_1/n_2}(\theta_1) = \frac{1}{2} \left[\frac{\tan^2(\theta_1 - \theta_2)}{\tan^2(\theta_1 + \theta_2)} + \frac{\sin^2(\theta_1 - \theta_2)}{\sin^2(\theta_1 + \theta_2)} \right]. \quad (18)$$

Equations (17) and (18) are symmetric with respect to θ_1 and θ_2 . Therefore, if θ_1 and θ_2 verify Eq. (17), we have

$$r_{n_1/n_2}(\theta_1) = r_{n_2/n_1}(\theta_2) \quad (19)$$

which means that the Fresnel reflection factor takes the same value if the light beam is transmitted from medium 1 to medium 2 as if it were transmitted from medium 2 to medium 1.

The ratio of incident intensity that is transmitted through the interface, called transmission factor, is also given by Fresnel's formulae. It is generally expressed as a function of the reflection factor, according to the principle of conservation of energy

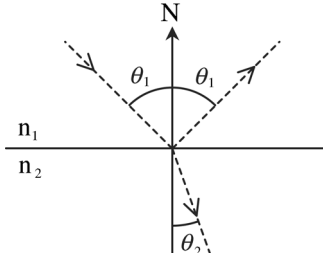


Figure 7. Reflection and refraction of a light ray at the interface of two different media ($n_2 > n_1$).

$$t_{n_1/n_2}(\theta_1) = 1 - r_{n_1/n_2}(\theta_1). \quad (20)$$

The transmission factor is also independent of which side of the interface the light is incident on.

Internal Reflection of Diffuse Incident Light on an Interface: Judd's Diffuse Internal Reflectance.

The aim of this section is to calculate the internal reflectance of an interface, i.e., to specify, for diffuse incident light, the ratio of incident irradiance that is reflected by the interface.

A source S of irradiance E_i , located in medium 2, is assumed to be a Lambertian emitter. It emits a radiance E_i/π , independent of direction. We can express this radiance as a function of the flux $d^2\Phi$ emitted by an element of surface ds_s of normal \mathbf{N} through a solid angle $d\omega_s$ oriented in a direction (θ, ϕ) .

$$\frac{E_i}{\pi} = \frac{d^2\Phi}{d\omega_s ds_s \cos\theta} \quad (21)$$

The solid angle $d\omega_s$ subtends a portion of area ds of the interface's surface (Fig. 8). If P is a point of ds , we call $d\omega$ the solid angle subtended by the projected area $ds_s \cos\theta$ at point P . Thus, thanks to the radiance invariance property (Eq. 3),

$$\frac{E_i}{\pi} = \frac{d^2\Phi}{d\omega ds \cos\theta}. \quad (22)$$

The flux incident to the interface is therefore

$$d^2\Phi = \frac{E_i}{\pi} d\omega ds \cos\theta. \quad (23)$$

A ratio $r_{n_2/n_1}(\theta)$ (Fresnel reflection factor, Eq. 18) of this incident flux $d^2\Phi$ is internally reflected by the interface. According to the Snell's laws, the reflection angles equal the incidence angles θ and ϕ , and thus the reflected solid angle equals the incident solid angle $d\omega$. The reflected flux $d^2\Phi_r$ is

$$d^2\Phi_r = r_{n_2/n_1}(\theta) d^2\Phi = r_{n_2/n_1}(\theta) \frac{E_i}{\pi} d\omega ds \cos\theta \quad (24)$$

The quantity $d^2\Phi_r/ds$ is an element of irradiance. If we replace $d\omega$ by $\sin\theta d\theta d\phi$ (above), we have

$$\frac{d^2\Phi_r}{ds} = r_{n_2/n_1}(\theta) \frac{E_i}{\pi} \cos\theta \sin\theta d\theta d\phi. \quad (25)$$

By integrating this quantity over the hemisphere, we obtain the irradiance E internally reflected by the interface

$$E = \int_0^{2\pi} \int_0^{\pi/2} r_{n_2/n_1}(\theta) \frac{E_i}{\pi} \cos\theta \sin\theta d\theta d\phi. \quad (26)$$

The integration over ϕ yields a factor 2π (since the terms inside the integral are independent of ϕ), the term $\cos\theta \sin\theta$ can be replaced by $\sin(2\theta)/2$, and the constant E_i can be extracted from the integral. The radiance internally reflected by the interface is therefore

$$E = E_i \int_0^{\pi/2} r_{n_2/n_1}(\theta) \sin 2\theta d\theta. \quad (27)$$

The ratio E/E_i gives the internal reflectance r_i of the interface

$$r_i = \int_0^{\pi/2} r_{n_2/n_1}(\theta) \sin 2\theta d\theta. \quad (28)$$

In the case of a coated Lambertian substrate, the source S models the light sent by the substrate, and r_i gives the ratio of light that is internally reflected upon the coating-air interface. Judd¹ computed the value of r_i as a function of the coating's refractive index n_2 for $n_1 = 1$ (air) by applying a discrete version of Eq. (28).

Transmission of Light Through an Interface. The transmission of light through an interface is expressed differently according to whether we consider radiances or irradiances. We deal with irradiances when we are interested in calculating the ratio of diffuse incident light that is transmitted through the interface. By definition, the ratio of transmitted to incident irradiances is given by the transmittance of the interface. If the coated layer is non-absorbent, according to the principle of conservation of energy the incident irradiance E_i is decomposed into a reflected irradiance $r_i E_i$ where the interface internal reflectance r_i is given by Eq. (28), and a transmitted irradiance, $t_i E_i$. This yields the following relation between the reflectance of the interface and its transmittance

$$t_i = 1 - r_i. \quad (29)$$

When the transmitted light is captured from within a given solid angle, we deal rather with radiances. The transmission through the interface is characterized by the ratio of transmitted to incident radiances, which includes, in addition to the ratio of transmitted light (Fresnel transmission factor), the effect of refraction of the pencil of rays on the solid angles (cone spreading).

We consider a small surface of the interface, of area ds , receiving a light flux $d^2\Phi_2$ contained into a solid angle $d\omega_2$ around direction (θ_2, ϕ_2) . The corresponding radiance $L_2^{(\theta_2, d\omega_2; ds)}$ (Eq. 5) is

$$L_2^{(\theta_2, d\omega_2; ds)} = \frac{d^2\Phi_2}{d\omega_2 ds \cos\theta_2}. \quad (30)$$

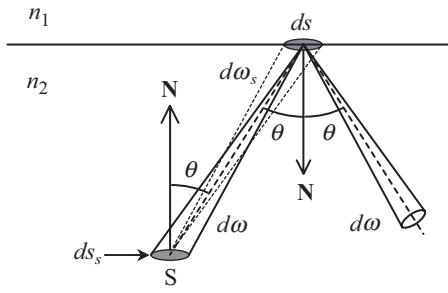


Figure 8. Reflection of a diffuse pencil of light onto the interface between two media of different refractive indices.

A ratio $1 - r_{n_2/n_1}(\theta_2)$ (Fresnel transmission factor, Eq. 20) of the flux $d^2\Phi_2$ is transmitted into medium 1 in direction θ_1 related to θ_2 by Snell's law (Eq. 17). The transmitted flux $d^2\Phi_1$ is therefore

$$d^2\Phi_1 = [1 - r_{n_2/n_1}(\theta_2)] d^2\Phi_2. \quad (31)$$

We call $L_1^{(\theta_1, d\omega_1; ds)}$ the transmitted radiance, corresponding to the element of flux, $d^2\Phi_1$, emerging from ds and contained into a solid angle, $d\omega_1$ (different from $d\omega_2$ due to the refraction) around the direction (θ_1, ϕ_1) (Fig. 9)

$$L_1^{(\theta_1, d\omega_1; ds)} = \frac{d^2\Phi_1}{d\omega_1 ds \cos \theta_1} \quad (32)$$

A combination of Eqs. (30), (31) and (32) gives the following ratio between the transmitted and incident radiances,

$$\frac{L_1^{(\theta_1, d\omega_1; ds)}}{L_2^{(\theta_2, d\omega_2; ds)}} = [1 - r_{n_2/n_1}(\theta_2)] \frac{d\omega_2 \cos \theta_2}{d\omega_1 \cos \theta_1},$$

where the solid angles can be written under the form $d\omega = \sin \theta d\theta d\phi$ (Eq. 3). We know, according to Snell's first law, that the light transmitted through a horizontal plane does not undergo any azimuthal deviation, i.e., $d\phi_1 = d\phi_2$. Therefore,

$$\frac{L_1^{(\theta_1, d\omega_1; ds)}}{L_2^{(\theta_2, d\omega_2; ds)}} = [1 - r_{n_2/n_1}(\theta_2)] \frac{\cos \theta_2 \sin \theta_2 d\theta_2}{\cos \theta_1 \sin \theta_1 d\theta_1}$$

The ratio, $\sin \theta_2 / \sin \theta_1$, is given directly by Eq. (17). By differentiating Eq. (17) we obtain

$$\cos \theta_2 d\theta_2 = \frac{n_1}{n_2} \cos \theta_1 d\theta_1.$$

By combining Eq. (17) with its differential form we have

$$\frac{\sin \theta_2 \cos \theta_2 d\theta_2}{\sin \theta_1 \cos \theta_1 d\theta_1} = \left(\frac{n_1}{n_2} \right)^2. \quad (33)$$

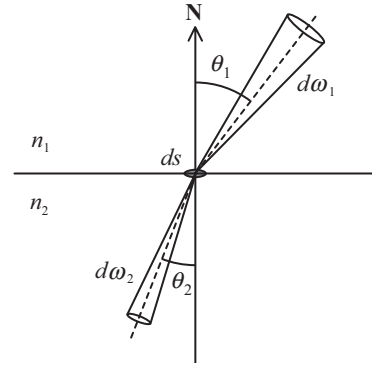


Figure 9. The light contained in a solid angle $d\omega_2$ in medium 2 is refracted into medium 1 within a solid angle $d\omega_1$ ($d\omega_2 < d\omega_1$ if $n_2 > n_1$).

Therefore, the ratio of the radiances at the interface between media 1 and 2 is

$$\frac{L_1^{(\theta_1, d\omega_1; ds)}}{L_2^{(\theta_2, d\omega_2; ds)}} = [1 - r_{n_2/n_1}(\theta_2)] \left(\frac{n_1}{n_2} \right)^2. \quad (34)$$

The term $(n_1/n_2)^2$, characteristic of the cone spreading, appears since the radiance is transmitted through an interface. For transmission of irradiance, the cone spreading is not taken into account, even for a thin pencil of light rays, since irradiance ignores the spatial distribution of the light.

Reflectance of a Solid Layer on a Lambertian Substrate

In this section, we consider a layer of refractive index n_2 , in contact with a Lambertian substrate of reflectance ρ_B on the one side, and in contact with air on the other side. The substrate and the layer are assumed to have the same refractive index, which avoids any Fresnel reflection at the interface between the substrate and the layer. The interface between the layer and the air is a planar interface. The refractive index of air is assumed to be $n_1 = 1$. The relative refractive indices of the interfaces n_2/n_1 (layer to air) and n_1/n_2 (air to layer) become respectively n_2 and $1/n_2$.

Reflectance of a Transparent Layer on a Lambertian Substrate. A collimated light beam, of irradiance E_i , arrives onto the air side of the interface with an incidence angle θ_1^i (Fig. 10). A proportion $r_{n_1/n_2}(\theta_1^i)$ of the incident light, which is equal to $r_{n_2}(\theta_1^i)$, is reflected into the air along the specular direction. Since the detector is not placed in the specular direction, this external specular reflection is neglected.

The beam penetrates the layer with a transmission factor $1 - r_{n_2}(\theta_2^i)$ (Eqs. 19 and 20) and propagates into the layer with a refraction angle θ_2^i (Eq. 17) until reaching the Lambertian substrate. The substrate, which reflects uniformly over the whole hemisphere a ratio ρ_B of the incident irradiance,

$$[1 - r_{n_2}(\theta_2^i)] E_i,$$

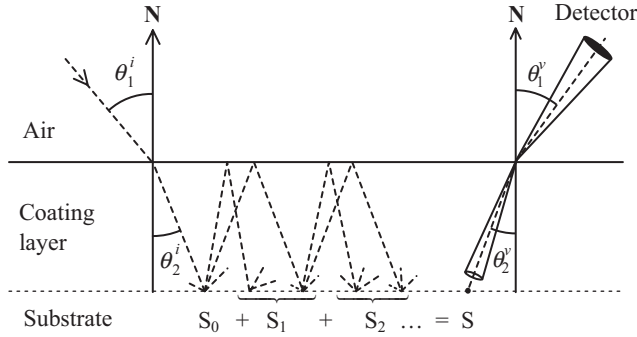


Figure 10. Path of the light from the source (collimated beam) to the detector, with multiple internal reflections. The light reflected by the substrate after having been internally reflected k times by the interface is thought to be a source S_k .

can be modeled as a diffuse source S_0 of irradiance

$$E_0 = \rho_B \left[1 - r_{n_2}(\theta_2^i) \right] E_i.$$

A ratio r_i of the irradiance E_0 is internally reflected on the coating-air interface back into the substrate. The substrate reflects uniformly over the whole hemisphere a ratio ρ_B of its received irradiance $r_i E_0$. Hence, after one internal reflection, the substrate can be modeled as a diffuse source S_1 of irradiance

$$E_1 = \rho_B r_i E_0.$$

Then, the light is reflected alternately by the interface and by the substrate. After k internal reflections, the substrate re-emits diffuse light like a source S_k of irradiance

$$E_k = (\rho_B r_i)^k E_0 = \left[1 - r_{n_2}(\theta_2^i) \right] \rho_B (\rho_B r_i)^k E_i.$$

By summing the contributions of the all sources S_k we obtain a single diffuse source S which models the light reflected by the substrate including the multiple internal reflections. Its irradiance E_S results from the geometric series

$$E_S = \left[1 - r_{n_2}(\theta_2^i) \right] \left(\rho_B \sum_{k=0}^{\infty} (\rho_B r_i)^k \right) E_i,$$

which converges towards

$$E_S = \left[1 - r_{n_2}(\theta_2^i) \right] \frac{\rho_B}{1 - \rho_B r_i} E_i.$$

The corresponding radiance L_S independent of direction since S is a Lambertian emitter (see Eq. 13), is

$$L_S = \frac{1}{\pi} E_S = \frac{1}{\pi} \left[1 - r_{n_2}(\theta_2^i) \right] \frac{\rho_B}{1 - \rho_B r_i} E_i. \quad (35)$$

Until now, we have just dealt with the portion of light that is internally reflected, without dealing with the por-

tion of light transmitted into air. For each ray incident to the interface from direction θ_2^v , we obtain the radiance of the light transmitted into air, i.e., toward the detector, by applying a factor

$$\left(1 - r_{n_2}(\theta_2^v) \right) (1/n_2)^2$$

to the incident radiance (see Eq. 34). It is equivalent, by factorization, to apply this factor to the sum of the all incident rays (coming from direction θ_2^v), whose radiance L_S is expressed by Eq. (35). Hence, the radiance of the light transmitted into the air along direction θ_1^v , i.e., captured by the detector, is

$$L^{(\theta_1^v)} = \left[1 - r_{n_2}(\theta_2^i) \right] \left[1 - r_{n_2}(\theta_2^v) \right] \left(\frac{1}{n_2} \right)^2 \frac{\rho_B}{1 - \rho_B r_i} \frac{E_i}{\pi}. \quad (36)$$

Considering the radiance $L_{ref}^{(\theta_1^v)}$ that would be reflected by a perfect white diffuse reflector illuminated with an irradiance E_i (see Eq. 13)

$$L_{ref}^{(\theta_1^v)} = E_i / \pi \quad (37)$$

the ratio $L^{(\theta_1^v)} / L_{ref}^{(\theta_1^v)}$ gives the reflectance factor R_{TL} of the substrate coated with a transparent layer

$$R_{TL} = \left[1 - r_{n_2}(\theta_2^i) \right] \left[1 - r_{n_2}(\theta_2^v) \right] \left(\frac{1}{n_2} \right)^2 \frac{\rho_B}{1 - \rho_B r_i}. \quad (38)$$

Equation (38) is the Shore and Spoonhower reflectance equation applied to the case of a transparent coating.³ It reproduces the Williams–Clapper model² if $\theta_1^i = 45^\circ$, $\theta_1^v = 0^\circ$ and $n_2 = 1.53$.

Williams and Clapper studied the case of $\rho_B = 1$ and $n_2 = 1.53$, and found that the reflectance of the coated substrate was $R_{TL} = 1$, i.e., all incident light is reflected. They interpreted this result as compensation between the effect of internal reflections and the effect of solid angle spreading. Shore and Spoonhower have shown recently that the compensation was accurate only for the particular $45^\circ/0^\circ$ geometry and the particular refractive index of 1.53.³

The Lambertian substrate coated with a transparent layer behaves nearly, but not exactly, as a Lambertian reflector. This can be verified by comparing the element of irradiance reflected by a perfect white diffuse reflector with and without coating. A perfect white diffuse reflector reflects a constant radiance E_i/π (Eq. 37) in every direction of the hemisphere; thus it reflects in a direction θ_1^v an element of irradiance,

$$dE_{ref}^{(\theta_1^v)} = \cos \theta_1^v d\omega E_i / \pi.$$

For a fixed solid angle, the plot of $dE_{ref}^{(\theta_1^v)}$ as a function of θ_1^v is a cosine curve (dashed line in Fig. 11, plotted for $d\omega = 1$ and $E_i/\pi = 1$) characteristic of a Lambertian reflector. The coated white diffuse reflector reflects the radiance $L^{(\theta_1^v)}$ depending on θ_1^v given by Eq. (36), and the element of irradiance $dE^{(\theta_1^v)} = L^{(\theta_1^v)} \cos \theta_1^v d\omega$. The curve of $dE^{(\theta_1^v)}$ as a function of θ_1^v (solid line in Fig. 11, for $\theta_1^i = 45^\circ$, $\rho_B = 1$, $n_2 = 1.53$, $d\omega = 1$ and $E_i/\pi = 1$) shows

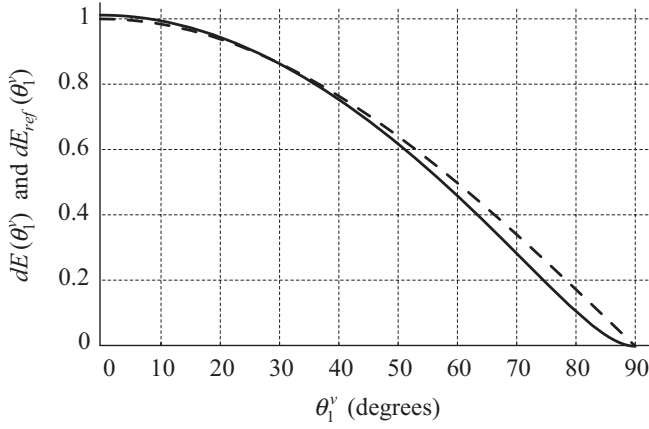


Figure 11. Evolution in function of the viewing angle θ_1^v of the element of irradiance reflected by coated (dE , solid line) and uncoated (dE_{ref} , dashed cosine curve) white diffuse reflectors.

that the coated diffuse reflector does not exactly follow Lambert's cosine law: the coated diffuse reflector appears darker than the uncoated reflector if the viewing angle is larger than 30° (ignoring the gloss due to external specular reflection).

Reflectance of a Colored Layer on a Lambertian Substrate: The Williams–Clapper Model. In this section, the substrate is coated with a colored layer, which absorbs light as a function of its wavelength λ . We call t_λ the transmittance of the layer along a single base-to-interface path normal to the base. In the previous section, we characterized the reflectance of a surface coated with a transparent layer ($t_\lambda = 1$). Here, we present an extension of Eq. (38) for a transmittance, $t_\lambda < 1$ considering any θ_1^i / θ_1^v geometries.

The transmittance of the layer depends on the length of the path traversed by the ray, according to the Beer–Lambert law.¹² The unit length is the length of a path along the normal \mathbf{N} of the interface. If the ray traverses the layer with an angle θ with respect to \mathbf{N} , the path length is $1/\cos\theta$ and the attenuation applied to the ray is $t_\lambda^{2/\cos\theta}$. Figure 12 shows the path length of rays entering, emerging from, and internally reflected into the colored layer.

We have seen above that the internal reflectance of the interface between the air and a transparent layer is r_i (Eq. 28). We may generalize the expression of r_i to an interface between the air and a colored layer of transmittance t_λ . Thus, we follow the same reasoning line as before. The generalization consists of inserting into Eq. (24) the transmittance term $t_\lambda^{2/\cos\theta}$ corresponding to a double path of length $1/\cos\theta$ within the coated layer

$$d^2\Phi_r = r_{n_2/n_1}(\theta) t_\lambda^{2/\cos\theta} d^2\Phi \quad (39)$$

According to the same considerations as for Eqs. (24) to (28), we obtain the internal reflectance $r_{i\lambda}$ of the interface between the air and a coated layer

$$r_{i\lambda} = \int_0^{\pi/2} t_\lambda^{2/\cos\theta} r_{n_2}(\theta) \sin 2\theta d\theta \quad (40)$$

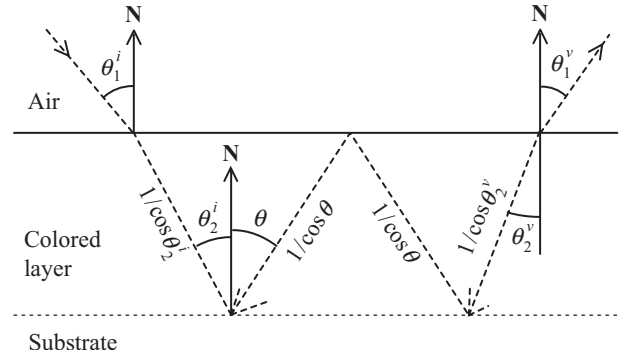


Figure 12. Path length of rays of light traversing a colored layer. The unit length corresponds to a path along the normal vector \mathbf{N} .

The print is illuminated by a collimated beam of irradiance E_i coming with an incident angle θ_1^i . The beam penetrates the colored layer with an angle θ_2^i and with a transmission factor $1 - r_{n_2}(\theta_2^i)$. After having traversed a path of length $1/\cos\theta_2^i$ within the colored layer, the light reaches the substrate with an irradiance

$$\left[1 - r_{n_2}(\theta_2^i)\right] t_\lambda^{1/\cos\theta_2^i} E_i.$$

A ratio ρ_B of this irradiance is diffused and reflected back by the substrate towards the interface. The irradiance E_0 received by the interface

$$E_0 = \rho_B \left[1 - r_{n_2}(\theta_2^i)\right] t_\lambda^{1/\cos\theta_2^i} E_i,$$

is internally reflected by the interface (in a proportion $r_{i\lambda}$) and then reflected back by the substrate (in a proportion ρ_B). The irradiance E_1 reflected by the substrate towards the interface after one internal reflection is therefore

$$E_1 = \rho_B r_{i\lambda} E_0,$$

and the irradiance E_k reflected by the substrate towards the interface after k internal reflections is

$$E_k = (\rho_B r_{i\lambda})^k E_0.$$

The total irradiance E_S reemitted by the substrate results from the sum of the all irradiances E_k yielding a geometric series

$$E_S = \left[1 - r_{n_2}(\theta_2^i)\right] t_\lambda^{1/\cos\theta_2^i} \rho_B \left(\sum_{k=0}^{\infty} (\rho_B r_{i\lambda})^k \right) E_i$$

which converges towards

$$E_S = \left[1 - r_{n_2}(\theta_2^i)\right] t_\lambda^{1/\cos\theta_2^i} \frac{\rho_B}{1 - \rho_B r_{i\lambda}} E_i$$

We now consider a ray of light emitted by the substrate in the direction θ_2^v . Since the substrate is Lambertian, the radiance of this ray is E_S/π . It reaches the interface with an attenuation factor $t_\lambda^{1/\cos\theta_2^v}$ due to the transmittance of the layer. The radiance $L_2^{(\theta_2^v)}$ incident onto the interface is therefore

$$L_2^{(\theta_2^v)} = \left[1 - r_{n_2}(\theta_2^i)\right] t_\lambda^{1/\cos\theta_2^i} t_\lambda^{1/\cos\theta_2^v} \frac{\rho_B}{1 - \rho_B r_{i\lambda}} \frac{E_i}{\pi}. \quad (41)$$

According to Eq. (34), the radiance $L_1^{(\theta_1^v)}$ transmitted through the interface into direction (θ_1^v, ϕ) and captured by the detector is

$$L_1^{(\theta_1^v)} = \left[1 - r_{n_2}(\theta_2^i)\right] \frac{1 - r_{n_2}(\theta_2^v)}{n_2^2} \frac{\rho_B t_\lambda^{1/\cos\theta_2^i + 1/\cos\theta_2^v}}{1 - \rho_B r_{i\lambda}} \frac{E_i}{\pi}. \quad (42)$$

Considering the radiance $L_{ref}^{(\theta_1^v)}$ that would be reflected by a perfect white diffuse reflector illuminated with an irradiance E_i (see Eq. 13)

$$L_{ref}^{(\theta_1^v)} = E_i/\pi, \quad (43)$$

the ratio $L^{(\theta_1^v)}/L_{ref}^{(\theta_1^v)}$ gives the reflectance factor R_{CL} of the substrate coated with a colored layer, for incident angle θ_1^i and viewing angle θ_1^v .

$$R_{CL} = \left[1 - r_{n_2}(\theta_2^i)\right] \frac{1 - r_{n_2}(\theta_2^v)}{n_2^2} \frac{\rho_B t_\lambda^{1/\cos\theta_2^i + 1/\cos\theta_2^v}}{1 - \rho_B r_{i\lambda}}. \quad (44)$$

This expression is presented in a similar form by Shore and Spoonhower.³ It reproduces the equation of Williams and Clapper for the special case of $n_2 = 1.53$, $\theta_2^i = 45^\circ$, and $\theta_2^v = 0^\circ$.

Reflectance of a Colored Layer on a Lambertian Substrate Measured with an Integrating Sphere Geometry. Shore and Spoonhower³ have generalized the Williams–Clapper model to the integrating sphere measurement geometry. In this geometry, the incident light is a collimated beam oriented with an angle θ_1^i in respect to N. The path of the light within the layered substrate is the same as above. However, in contrast to the detector which measures a radiance (the radiance $L_1^{(\theta_1^i)}$ detailed in Eq. 42), the integrating sphere measures an irradiance, i.e., it measures light emerging from the coated substrate in the all directions of the hemisphere.

The irradiance E emerging from the coated substrate can be derived from the radiance $L_1^{(\theta_1^i)}$ according to Eq. (7)

$$E = \int_0^{2\pi} \int_0^{\pi/2} L^{(\theta_1^i)} \cos\theta_1^v \sin\theta_1^v d\theta_1^v d\phi. \quad (45)$$

After inserting the expression of $L_1^{(\theta_1^i)}$ (Eq. 42) into Eq. (45), we obtain

$$E = \left[1 - r_{n_2}(\theta_2^i)\right] t_\lambda^{1/\cos\theta_2^i} \frac{\rho_B}{1 - \rho_B r_{i\lambda}} E_i \times \frac{1}{n_2^2} \int_0^{\pi/2} \left(1 - r_{n_2}(\theta_2^v)\right) t_\lambda^{1/\cos\theta_2^v} \cos\theta_1^v \sin\theta_1^v d\theta_1^v. \quad (46)$$

The integral in Eq. (46) gathers elements expressed according to two different variables (angles θ_1^v and θ_2^v). In order to express all elements according to the same variable, we refer to Eq. (33) where

$$\cos\theta_1^v \sin\theta_1^v d\theta_1^v = n_2^2 \cos\theta_2^v \sin\theta_2^v d\theta_2^v$$

and we obtain the following expression for the irradiance captured by the integrating sphere

$$E = \left[1 - r_{n_2}(\theta_2^i)\right] t_\lambda^{1/\cos\theta_2^i} \frac{\rho_B}{1 - \rho_B r_{i\lambda}} E_i \times \int_0^{\pi/2} \left(1 - r_{n_2}(\theta_2^v)\right) t_\lambda^{1/\cos\theta_2^v} \cos\theta_2^v \sin\theta_2^v d\theta_2^v. \quad (47)$$

Finally, the ratio E/E_i gives the reflectance as well as the reflectance factor of the coated substrate, since E_i is the incident irradiance as well as the irradiance that would be reflected by a perfect white diffuser. Therefore, the reflectance factor of the substrate coated with a colored layer measured with an integrating sphere is

$$R_{IS} = \left[1 - r_{n_2}(\theta_2^i)\right] \frac{\rho_B t_\lambda^{1/\cos\theta_2^i} t_{i\lambda}}{1 - \rho_B r_{i\lambda}} \quad (48)$$

with

$$t_{i\lambda} = \int_0^{\pi/2} \left(1 - r_{n_2}(\theta)\right) t_\lambda^{1/\cos\theta} \sin 2\theta d\theta. \quad (49)$$

Note that in Eq. (47), the factor n_2^2 , characteristic of cone spreading, has disappeared. It is thus confirmed that this factor appears only for radiance transfer through an interface, but not for irradiance transfer.

A further interesting point concerns the particular case of a transparent layer. By inserting $t_\lambda = 1$ into Eqs. (40) and (49), we have $r_{i\lambda} = r_i$ and $t_{i\lambda} = 1 - r_i$. Thus, Eq. (48) becomes

$$R_{IS} = \left[1 - r_{n_2}(\theta_2^i)\right] (1 - r_i) \frac{\rho_B}{1 - \rho_B r_i}. \quad (50)$$

The expression of R_{IS} corresponds to the Saunderson correction,⁸ for the case where the external specular reflection is discarded. The Saunderson correction corrects the reflectance ρ_B of a substrate in order to take into account multiple internal reflections at the interface between the air and the coating layer.

Reflectance of a Halftoned Layer on a Lambertian Substrate

Halftone Prints. In halftone prints, the substrate is coated with small ink dots, covering a fractional area a of the substrate surface. We consider a planar interface between the air and the substrate and we assume that the ink and the substrate have the same refractive index n_2 (Fig. 13).

The print is illuminated with a collimated beam oriented with an angle θ_1^i in respect to N. A ratio $r_{n_2}(\theta_2^i)$ is reflected specularly in the air and may either reach or

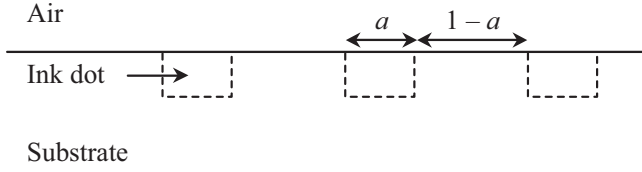


Figure 13. A half-tone print is made small ink dots, covering a fractional area a of the substrate surface.

not reach the detector. Factor K indicates if the detector captures the specular reflection ($K = 1$) or not ($K = 0$).

In contrast to the solid layer, the transmittance of the half-tone print varies as a function of the position. The position where the light enters the print and where it emerges has to be considered. It is necessary to model the lateral propagation of light within the print. Two classical approaches are based on opposite assumptions:

- Murray and Davies⁴ assumed that the lateral propagation of light within the substrate is far smaller than the printed dot size, i.e., light always emerges from the same colorant (paper or ink) as the colorant from which it enters. This model is not considered here since it does not take into account multiple internal reflections.
- Clapper and Yule⁵ assumed that the light propagation is considerably larger than the dot size, i.e., the probability of a light ray entering a given colorant and the probability of it exiting from a given colorant are completely uncorrelated.

Recently, reflectance models have been proposed where the probability of light exiting from a certain colorant depends on the distance light needs to propagate laterally to reach that colorant.^{6,7} However, these models are outside the scope of the present paper.

The Clapper–Yule Model. The model proposed by Clapper and Yule⁵ is initially adapted to an integrating sphere measurement geometry. This model can also be applied to a θ_1^i/θ_1^v geometry if specular surface reflections are discarded. Thus, we detail the case of the integrating sphere geometry, and then discuss the case of a θ_1^i/θ_1^v geometry.

The incident collimated light, of irradiance E_i enters the print with a Fresnel transmission factor $1 - r_{n_2}(\theta_2^i)$ either in a colored area (transmittance t_λ , probability a , where a is the fractional area covered by the ink dots) or in an uncolored area (transmittance 1, probability $1 - a$). It is then reflected by the substrate of reflectance ρ_B which reemits toward the interface an irradiance (Fig. 14)

$$E_0 = [1 - r_{n_2}(\theta_2^i)] \rho_B (1 - a + at_\lambda^2) E_i. \quad (51)$$

A ratio r_i of the irradiance E_0 is internally reflected at the interface (see Eq. 28), either at a colored area (probability a , transmittance t_λ^2 , owing to two passes through the ink layer) or at an uncolored area (probability $1 - a$, transmittance 1). The internally reflected light returns back into the substrate (reflectance ρ_B). The irradiance reemitted by the substrate toward the interface after one internal reflection is therefore

$$E_1 = r_i \rho_B (1 - a + at_\lambda^2) E_0$$

and the irradiance reemitted by the substrate toward the interface after k internal reflections is

$$E_k = \left(r_i \rho_B (1 - a + at_\lambda^2) \right)^k E_0.$$

The total irradiance E_S reemitted by the substrate towards the interface results from the sum of the all irradiances E_k yielding a geometric series

$$E_S = [1 - r_{n_2}(\theta_2^i)] \rho_B (1 - a + at_\lambda) \left(\sum_{k=0}^{\infty} \left(r_i \rho_B (1 - a + at_\lambda^2) \right)^k \right) E_i$$

which converges towards

$$E_S = [1 - r_{n_2}(\theta_2^i)] \frac{\rho_B (1 - a + at_\lambda)}{1 - r_i \rho_B (1 - a + at_\lambda^2)} E_i. \quad (52)$$

The irradiance E collected by the integrating sphere is

$$E = (1 - r_i) (1 - a + at_\lambda) E_S + K r_{n_2}(\theta_2^i) E_i \quad (53)$$

where $(1 - r_i)$ is the transmittance of the interface (recall the definition of transmittance above), $(1 - a + at_\lambda)$ expresses the weighted mean between the part of the light emerging from a colored area and the part of light emerging from a non colored area, and where $K r_{n_2}(\theta_2^i) E_i$ is the irradiance of the external specular reflection (see Eq. 19). After inserting Eq. (52) into Eq. (53) and dividing both members by E_i we obtain the reflectance ρ_{CY} of the half-tone print according to the Clapper–Yule model for the integrating sphere measuring geometry

$$\rho_{CY} = [1 - r_{n_2}(\theta_2^i)] \frac{(1 - r_i) \rho_B (1 - a + at_\lambda)^2}{1 - r_i \rho_B (1 - a + at_\lambda^2)} + K r_{n_2}(\theta_2^i). \quad (54)$$

Note that Eq. (54) also corresponds to the reflectance factor of a half-tone print measured by an integrating sphere using as reference a perfect white diffuser.

In their study, Clapper and Yule use as reference the unprinted substrate, i.e., paper coated with a transparent layer only; ρ_{ref} is derived from Eq. (54) by setting $a = 0$

$$\rho_{ref} = [1 - r_{n_2}(\theta_2^i)] \frac{(1 - r_i) \rho_B}{1 - r_i \rho_B} + K r_{n_2}(\theta_2^i). \quad (55)$$

Then, the ratio ρ/ρ_{ref} gives the reflection factor R_{CY} of the half-tone print for the integrating sphere geometry

$$R_{CY} = \frac{[1 - r_{n_2}(\theta_1^i)] \frac{(1 - r_i) \rho_B (1 - a + at_\lambda)^2}{1 - r_i \rho_B (1 - a + at_\lambda^2)} + K r_{n_2}(\theta_1^i)}{[1 - r_{n_2}(\theta_1^i)] \frac{(1 - r_i) \rho_B}{1 - r_i \rho_B} + K r_{n_2}(\theta_1^i)} \quad (56)$$

where the reference diffuse reflector used for calibrating the measuring instrument is the substrate coated with a transparent layer.

Equation (56) is in conformity with the formula developed by Clapper and Yule. If the external specular reflection is discarded from the measure ($K = 0$), Eq. (56) gives a simpler expression of R_{CY}

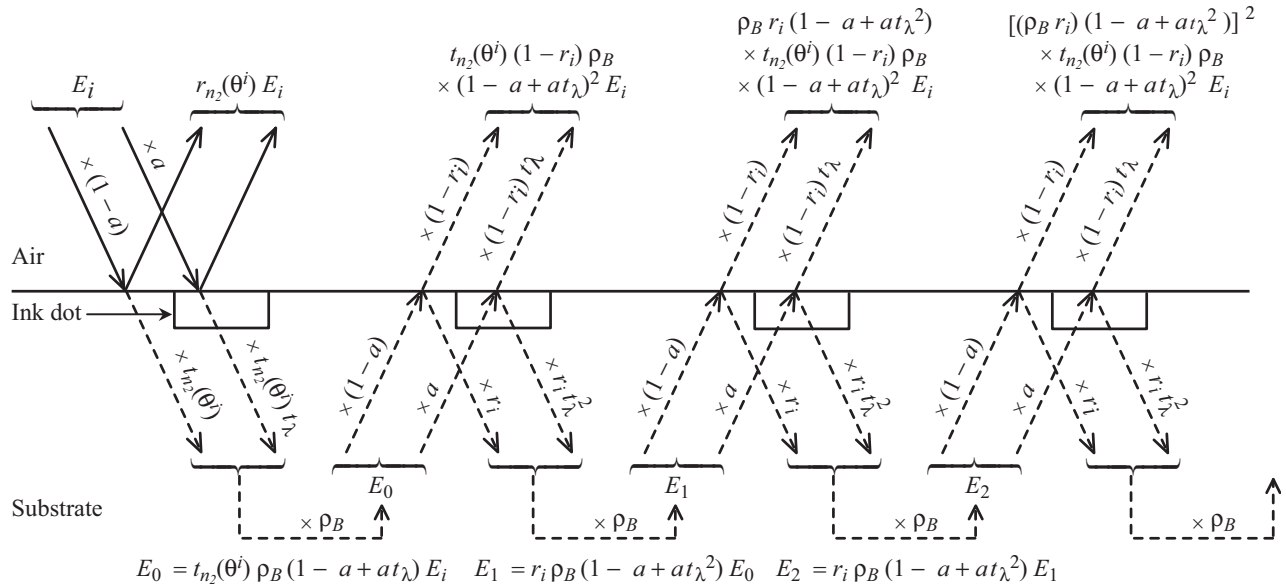


Figure 14. Internal reflections within a halftone print: E_i is the incident irradiance, E_k the irradiance reflected by the substrate after k internal reflections onto the interface ($k = 0, 1, \dots$) and dashed arrows represent diffuse light fluxes.

$$R_{CY} = \frac{(1 - r_i \rho_B)(1 - a + at_\lambda)^2}{1 - r_i \rho_B(1 - a + at_\lambda^2)}. \quad (57)$$

We can show that Eq. (57) is also valid for a θ_1^i/θ_1^v measurement geometry if it excludes the specular component ($K = 0$). The radiance $L_1^{(\theta_1^i)}$ perceived by the detector, oriented with an angle θ_1^v in respect to \mathbf{N} , depends on the radiance E_S/π (with E_S given by Eq. 52) that is incident to the substrate side of the interface and the attenuation applied to this irradiance while passing through the ink dots (factor $1 - a + at_\lambda$) and through the interface (factor $[1 - r_{n_2}(\theta_2^v)]/n_2^2$).

$$L^{(\theta_1^v)} = \frac{1 - r_{n_2}(\theta_2^v)}{n_2^2} (1 - a + at_\lambda) \frac{E_S}{\pi} \quad (58)$$

After inserting Eq. (52) into Eq. (58) we obtain the reflectance

$$\rho = \frac{1}{\pi} \left[1 - r_{n_2}(\theta_2^i) \right] \frac{1 - r_{n_2}(\theta_2^v)}{n_2^2} \cdot \frac{\rho_B (1 - a + at_\lambda)^2}{1 - r_i \rho_B (1 - a + at_\lambda^2)} \quad (59)$$

and the reference reflectance corresponding to the reflectance of the paper coated with a transparent layer (Eq. 59 with $a = 0$).

$$\rho_{ref} = \frac{1}{\pi} \left[1 - r_{n_2}(\theta_2^i) \right] \frac{1 - r_{n_2}(\theta_2^v)}{n_2^2} \cdot \frac{\rho_B}{1 - r_i \rho_B}$$

The ratio ρ/ρ_{ref} thus obtained yields the same result as Eq. (57). Therefore, the expression of the halftone print reflectance factor does not depend on the measurement geometry, provided that the specular component is not captured and that the unprinted substrate is chosen as reference reflector.

If the reference reflector is a perfect white diffuser ($\rho_{ref} = 1/\pi$), the reflectance factor of the halftone print for a θ_1^i/θ_1^v geometry is given by suppressing the factor $1/\pi$ in Eq. (59).

An interesting point to discuss is the special case of a solid layer ($a = 1$). We could expect the Williams–Clapper model to be a particular case of the Clapper–Yule model, but it is not exactly. For the integrating sphere geometry excluding the external specular reflection, the reflectance factor predicted by the Clapper–Yule model (Eq. 54 with $a = 1$ and $K = 0$) is

$$R_{CY(a=1)} = \left[1 - r_{n_2}(\theta_2^i) \right] \frac{\rho_B t_\lambda^2 (1 - r_i)}{1 - \rho_B t_\lambda^2 r_i} \quad (60)$$

whereas the reflectance factor predicted by the Williams–Clapper model (Eq. 48) is

$$R_{IS} = \left[1 - r_{n_2}(\theta_2^i) \right] \frac{\rho_B t_\lambda^{1/\cos\theta_2^i} t_{i\lambda}}{1 - \rho_B r_{i\lambda}}. \quad (61)$$

The difference between Eq. (60) and Eq. (61) is due to the fact that Clapper and Yule do not take into account the oblique paths within the colored layer, assuming that they induce a non significant error.⁵ Reasoning along this line, Eq. (60) can be derived from Eq. (61) if the three following approximations are admitted

- (i) $t_\lambda^{1/\cos\theta_2^i} \approx t_\lambda$
- (ii) $r_{i\lambda} \approx t_\lambda^2 r_i$
- (iii) $t_{i\lambda} \approx t_\lambda (1 - r_i)$

where r_i , $r_{i\lambda}$ and $t_{i\lambda}$ are detailed respectively in Eq. (28), (40) and (49). The detailed form of these approximations

$$\begin{aligned}
\text{(i)} \quad & t_\lambda^{1/\cos\theta_2^i} \approx t_\lambda \\
& r_{i\lambda} = \int_0^{\pi/2} t_\lambda^{2/\cos\theta} r_{n_2}(\theta) \sin 2\theta d\theta \\
\text{(ii)} \quad & \approx t_\lambda^2 \int_0^{\pi/2} r_{n_2}(\theta) \sin 2\theta d\theta = t_\lambda^2 r_i \\
& t_{i\lambda} = \int_0^{\pi/2} t_\lambda^{1/\cos\theta} (1 - r_{n_2}(\theta)) \sin 2\theta d\theta \\
\text{(iii)} \quad & \approx t_\lambda \int_0^{\pi/2} (1 - r_{n_2}(\theta)) \sin 2\theta d\theta = t_\lambda (1 - r_i)
\end{aligned}$$

makes explicit the omission of the exponent $1/\cos\theta$, which is characteristic of oblique paths.

The plots in Fig. 15 compare the evolution of the Clapper–Yule ($R_{CY(a=1)}$) and Williams–Clapper (R_{IS}) reflectance factors as functions of the value of the transmittance t_λ . For every t_λ value between 0 and 1, the approximations of Eq. (62) induce an overestimation of the print reflectance factor. For $t_\lambda = 0.78$, $R_{CY(a=1)}$ is 27.4% higher than R_{IS} (maximum error).

Conclusions

By following a radiometric approach in deriving the mathematical expressions for the Williams and Clapper and Clapper and Yule models, we try to give a more profound understanding of the physical phenomena involved. In particular, we model the reflectance of a coated color layer on top of a diffuse substrate by considering as input a collimated light beam having a given irradiance, computing the irradiance transmitted into the interface, and summing up all irradiance components diffusely reflected by the substrate and internally reflected by the interface. The transmitted output radiance (in the case of a θ^i/θ^v measuring geometry) or output irradiance (in the case of an integrating sphere) can then be easily derived from the sum of irradiance components incident to the layer-air interface. The ratio of output to input radiance or irradiances yields the reflectance. The reflectance factor is the relationship between this reflectance and the reflectance of a white diffuser. Such an approach allows us to derive and adapt the Williams and Clapper and Clapper and Yule models for various measuring geometries and for different reference white diffuse reflectors (coated paper, perfect white diffuser). In addition, by comparing the Williams and Clapper and Clapper and Yule models, we show that the Clapper and Yule model makes the simplifying assumption that the path of light across the colored medium has a length corresponding to the vertical thickness of that medium, and that its predictions consequently

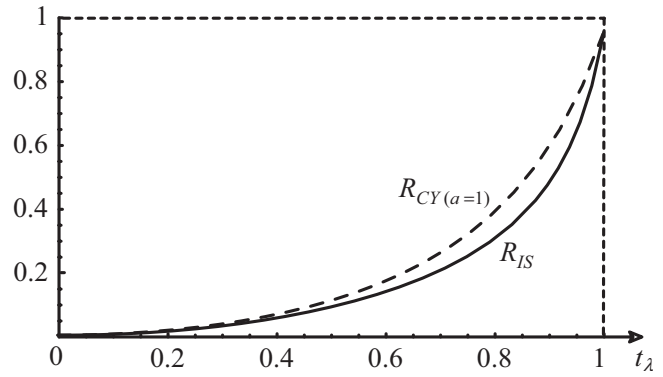


Figure 15. Clapper–Yule reflectance factor $R_{CY(a=1)}$ (dashed line), and Williams–Clapper reflectance factor R_{IS} (solid line) as a function of the layer transmittance t_λ , for the integrating sphere geometry with $\theta_1^i = 45^\circ$, $n_2 = 1.53$ and $\rho_B = 1$.

tend to overestimate the print reflectance factors. In future work, we intend to extend with the radiometric approach presented and establish models which are also capable of predicting the radiance or irradiance transmitted across a coated diffuse substrate. \blacktriangle

References

1. D. B. Judd, Fresnel reflection of diffusely incident light, *J. Natl. Bur. Standards* **29**, 329 (1942).
2. F. C. Williams and F. R. Clapper, Multiple internal reflections in photographic color prints, *J. Opt. Soc. Amer.* **29**, 595 (1953).
3. J. D. Shore and J. P. Spoonhower, Reflection density in photographic color prints: Generalizations of the Williams–Clapper transform, *J. Imaging Sci. Technol.* **45**(5), 484 (2001).
4. A. Murray, Monochrome reproduction in photoengraving, *J. Franklin Inst.* **221**, 721 (1936).
5. F. R. Clapper and J. A. C. Yule, The effect of multiple internal reflections on the densities of halftone prints on paper, *J. Opt. Soc. Amer.* **43**, 600 (1953).
6. P. Emmel and R. D. Hersch, A unified model for color prediction of halftoned prints, *J. Imaging Sci. Technol.* **44**(4), 351 (2000).
7. G. Rogers, A generalized Clapper–Yule model of halftone reflectance, *Color Res. Appl.* **25**(6), 402 (2000).
8. J. L. Saunderson, Calculation of the color of pigmented plastics, *J. Opt. Soc. Amer.* **32**(4), 727 (1942).
9. W. R. McCluney, *Introduction to Radiometry and Photometry*, Artech House, 1994, pp. 7–13.
10. G. Bruhat, *Optique*, 6th ed., Masson, 1992, p. 1004 (in French).
11. M. Born and E. Wolfe, *Principles of Optics*, 6th ed., Pergamon Press, Oxford, 1987, Sec. 1.5.
12. H.-H. Perkampus, *Encyclopedia of Spectroscopy*, VCH, Weinheim, 1995.
13. F. R. Ruckdeschel and O. G. Hauser, Yule–Nielsen effect in printing: A physical analysis, *Appl. Opt.* **17**, 3376 (1978).